Journal of Nano- and Electronic Physics
Vol. **12** No 2, 02005(5pp) (2020)

Журнал нано- та електронної фізики
Том **12** № 2, 02005(5cc) (2020)

Synthesis and Photodetection Properties of Sonochemically Exfoliated $Cu_{0.2}Sn_{0.8}Se$ Nanoparticles

Kunjal Patel*, G.K. Solanki, K.D. Patel, V.M. Pathak, Payal Chauhan, Anand Patel

Department of Physics, Sardar Patel University, Vallabh Vidyanagar, 388120 Gujarat, India

(Received 15 February 2020; revised manuscript received 12 April 2020; published online 25 April 2020)

Transition metal chalcogenides (TMCs) with atomically minute structure have shown excessive potential for their optoelectronics field applications and their counterparts. TMCs unique layer dependent properties have pinched increasing consideration of scientists. Here, the high yield synthesis of atomically minute $Cu_{0.2}Sn_{0.8}Se$ nanoparticles has been reported. The nanoparticles are synthesised by sonochemical exfoliation technique. The exfoliated $Cu_{0.2}Sn_{0.8}Se$ nanoparticles have orthorhombic lattice structure which is confirmed from powder X-ray Diffraction with P_{nma} space group. The lateral morphology of the as-synthesized nanoparticles examined under transmission electron microscopy showed them to be of uniform spherical shape. The selected area electron diffraction showed a spot pattern stating the particles to be single crystalline. Moreover, the photodetector based on $Cu_{0.2}Sn_{0.8}Se$ nanoparticles thin film is fabricated. The periodic 670 nm laser illumination of power intensity 3 mW/cm^2 is used to study the detector properties. The enhanced photo responsivity and specific detectivity is observed along with fast response. The outstanding detection properties are revealed from the responsivity, specific detectivity, and external quantum efficiency (EQE) of $Cu_{0.2}Sn_{0.8}Se$ nanoparticles-based photodetector.

Keywords: Exfoliation, Nanoparticles, Photodetector, Response time.

DOI: 10.21272/jnep.12(2).02005 PACS numbers: 61.46.Df, 78.67.Bf

1. INTRODUCTION

Group IV-VI compounds are found to own outstanding electronic and optoelectronic properties, whose applications are found in multiple exciton photovoltaic cells, thermoelectric cells field-effect transistors, topological insulators and phase-change memory [1-5]. Along with their bulk form, a substantial amount of low-dimensional metal chalcogenides semiconductor compounds have been synthesized via various chemical or physical methods [3,5-12]. Corresponding devices demonstrates significantly improved properties due to their small size, high surface-to-volume ratio and quantum confinement effects which mainly benefited from the low-scattering transport path of the carriers provided by the high aspect ratios, as well as the discrete energy states of the electron and hole induced by the spatial confinement [13-19]. Among them, tin (II) selenide (SnSe) is a distinctive p-type semiconductor material possesing a narrow direct band gap of ~ 1.30 eV and indirect bandgap of ~ 0.90 eV at room temperature [20]. Also, SnSe assumes a specific layered crystal structure in which non covalent force weakly bonds the neighbouring layers together [21, 22]. SnSe belongs to the IV-VI group layered semiconductor compounds. SnSe crystallises in an orthorhombic structure, but it undergoes transformation into tetragonal or cubic structures at high temperatures below its melting point of 860 °C [23]. However, the cubic structure of SnSe has been reported by a few groups [23-25] both in a nanocrystalline [26] and thin-film form [23, 24] even at low temperatures. Recently, inspired by its layered structure, narrow bandgap and some other advantages, including chemical stability and natural abundance, SnSe nanomaterial have drawn researchers interests intensely. Various SnSe nanostructures, including thin films [22, 27], nanocrystals [28], and layered nanosheets [29], have been explored. However, very few works on the synthesis SnSe nanostructure arrays in one-dimensional (1D) have been reported, and most of them implements chemical solution method [21, 27]. Photodetectors are sensors that detect photons (or electromagnetic waves) and transfer them to electric signals. According to the wavelength of the responsive spectra, photodetectors can work at UV (ultraviolet, 10-300 nm), visible (400-700 nm), IR (infrared, 700 nm-1 mm), and THz (0.1 to 1 mm, or 0.3 to 30 THz) ranges with various applications that play indispensable roles in our daily life [30-32]. Here, we present a photodetector based on $Cu_{0.2}Sn_{0.8}Se$ nanoparticles. Recently, chemical exfoliation technique has been proven to be the most convenient path due to readily available solvents like NMP, DMF, acetone, water, etc. [33-37]. Herein, $Cu_{0.2}Sn_{0.8}Se$ nanoparticles are synthesised in high yield by sonochemical exfoliation technique. We also demonstrate the more straightforward and large-area fabrication process for photodetector based on exfoliated nanoparticles using simple experimental procedure. The photodetector showed excellent response towards illumination.

2. EXPERIMENTAL

2.1 Sono-chemical Exfoliation of $Cu_{0.2}Sn_{0.8}Se$ Nanoparticles

The high yield synthesis of $Cu_{0.2}Sn_{0.8}Se$ nanoparticles began with sonochemical exfoliation technique. The $Cu_{0.2}Sn_{0.8}Se$ bulk compound powder have been grinded by the means of mortar pestle for 30 min to start the synthesis process. A mixture of 10 ml acetone and water was used as a solvent to disperse 50 mg

* kunjal_92@yahoo.com

powder of $Cu_{0.2}Sn_{0.8}Se$ nanoparticles. Then, the solution was sonicated for 8 h at a constant temperature of 20 °C using bath sonicator with 40 kHz frequency and 40 % amplitude. A brown dark coloured suspension of $Cu_{0.2}Sn_{0.8}Se$ nanoparticles was yielded by this process, containing exfoliated $Cu_{0.2}Sn_{0.8}Se$ nanoparticles and unexfoliated sediments. For the separation of nanoparticles, the suspension of $Cu_{0.2}Sn_{0.8}Se$ nanoparticles in acetone and water is centrifuged at 4000 rpm for 20 min, and finally, the supernatant was collected using micro-pipette for characterisation and fabrication of photodetectors. Finally, 10 ml suspension is dried and the exfoliated $Cu_{0.2}Sn_{0.8}Se$ nanoparticles are collected.

2.2 Material Characterization

The chemical confirmation and purity of $Cu_{0.2}Sn_{0.8}Se$ nanoparticles were investigated by energy dispersive analysis of X-ray (Field Emission Gun Scanning Electron Microscopy (FEG-SEM) with EDAX Make: FEI Ltd Model: Nova Nano SEM 450). The structural phase of bulk and atomically thin $Cu_{0.2}Sn_{0.8}Se$ nanoparticles were studied by powder X-ray diffraction technique using Bruker D8 advance diffractometer using CuK_{α} (1.5498 Å) radiation. The lateral morphology of nanoparticles is studied by Philips Tecnai 20 Transmission electron microscope operated at 200 keV electron beam. The particle size is obtained using High-Performance Particle size Analyzer with Zeta potential (Model: SZ100 Nanopartica; Make: Horiba, Japan).

2.3 Fabrication of Photodetector

A glass substrate of 1 cm^2 is nominated for the fabrication of photodetector. Then, the suspension of $Cu_{0.2}Sn_{0.8}Se$ nanoparticles is several times drop-casted on a glass substrate. Acetone and water were removed by continuous heating at 40 °C. For confirming the complete removal of acetone and water traces, the prepared device was annealed at 200 °C for 3 h. Then, the sensor is mounted on the Printed Circuit Board (PCB). The current-voltage characteristics in bias range ± 1.5 V in dark condition and illuminated condition is carried out for electrical measurments with Keithly-4200 SCS. At constant bias voltage of 1.5 V and under illuminated by 670 nm laser of power intensity 3 mW/cm^2 the transient photoresponse of fabricated device is recorded.

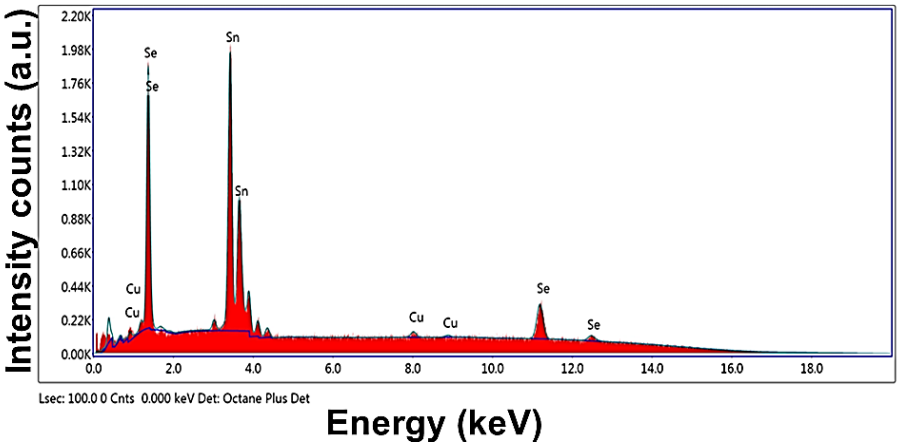

Fig. 1 – EDAX spectra of $Cu_{0.2}Sn_{0.8}Se$ nanoparticles

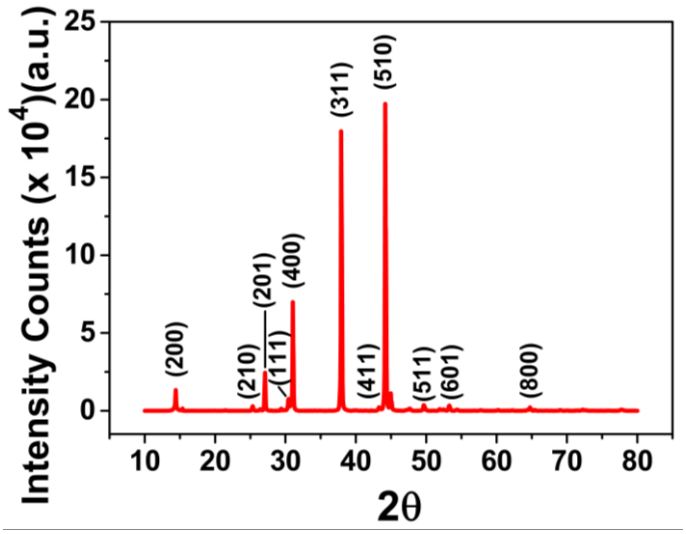

Fig. 2 – Powder XRD pattern of $Cu_{0.2}Sn_{0.8}Se$ nanoparticles

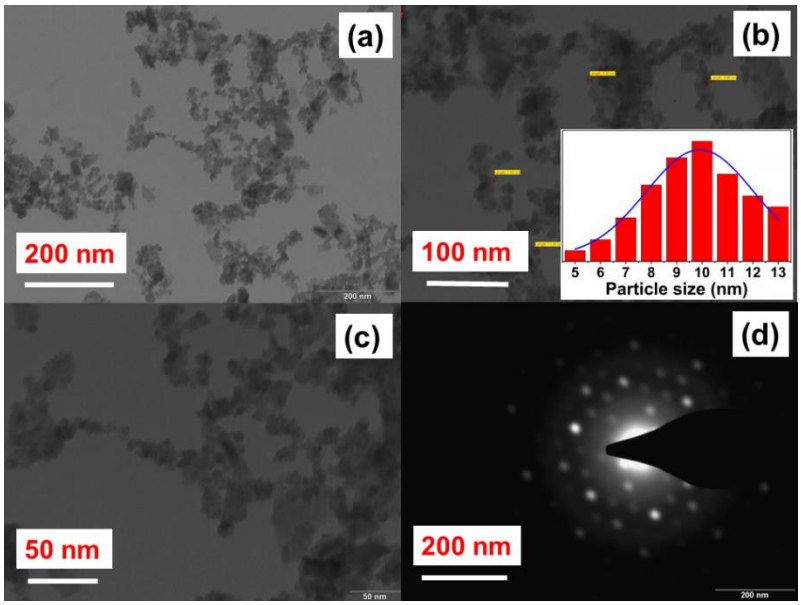

Fig. 3 – (a-c) TEM images of $Cu_{0.2}Sn_{0.8}Se$ nanoparticles (inset of Fig. 3 (b) is particle size distribution histogram) and (d) SAED pattern taken from $Cu_{0.2}Sn_{0.8}Se$ nanoparticles

3. RESULTS AND DISCUSSION

The sonochemical exfoliation technique for the synthesis of $Cu_{0.2}Sn_{0.8}Se$ nanoparticles is adopted. The solvent/sonicating medium, power and frequency of sonicator, the temperature of the solvent, sonication time, etc. are the parameters which affect the quality and yield of nanoparticles [38]. The chemical composition and purity of $Cu_{0.2}Sn_{0.8}Se$ nanoparticles are examined using energy dispersive analysis of X-ray (EDAX). As shown in Fig. 1, EDAX spectrum shows the peaks for 'Sn',' Se' and 'Cu' and no extra peaks are observed, attributing the purity of nanoparticles. The weight (%) of Sn, Se and Cu is found to be about 44.58 %, 53.71 % and 1.71 %, respectively. The atomic (%) of Sn, Se and Cu are found to be about 34.69 %, 62.83 % and 2.49 %, respectively. The results are also attributed to the stoichiometric composition of $Cu_{0.2}Sn_{0.8}Se$ nanoparticles. The structural investigation of the exfoliated $Cu_{0.2}Sn_{0.8}Se$ nanoparticles is accomplished by powder XRD technique using CuK_{α} radiation, as shown in Fig. 2. The sharp peaks found within the patterns indicate accurate and high crystallinity of the samples with (510) as the dominant peak. $Cu_{0.2}Sn_{0.8}Se$ nanoparticles adopt an orthorhombic structure within layers having space group P_{nma} having lattice parameters $a = 11.50$ Å, $b = 4.440$ Å and $c = 4.135$ Å. From the outcomes of X-ray Diffractogram, the accidental growth of secondary phase or impurity phase is absolutely ruled out. The sharp peaks in Fig. 2 for exfoliated sample are attributing the highly crystalline nature. Moreover, Transmission Electron Microscopy (TEM) is employed to study the lateral morphology of $Cu_{0.2}Sn_{0.8}Se$ nanoparticles in which large quantity of nanoparticles having various lateral dimensions are observed as shown in Fig. 3(a-c). Nanoparticles of particle dimension fall in the range from 5 nm to 13 nm as shown in particle size distribution histogram in the inset of Fig. 3(b). These particles have excellent dispersibility. The SAED pattern shows the single-crystalline nature of nanoparticles, as shown in Fig. 3(d).

The photodetection property of $Cu_{0.2}Sn_{0.8}Se$ nanoparticles thin film-based photodetector is exploited for their intended application in optoelectronics. The schematic diagram of photodetector based on $Cu_{0.2}Sn_{0.8}Se$ nanoparticles is shown in Fig. 4(a). Inset (i) shows the surface of the nanoparticle thin film (ii) shows cross-sectional image of the film. The smooth surface of the prepared film is seen from the SEM image in inset (i) and thickness of the film is scaled to be 9 μm which is found using the cross-sectional image of the prepared film. The electrical measurements began with current-voltage characteristics measurements in the dark and illuminated condition, as shown in Fig. 4(b). The exact ohmic behaviour of contacts between $Cu_{0.2}Sn_{0.8}Se$ nanoparticles and Ag electrode, i.e. Ag/ $Cu_{0.2}Sn_{0.8}Se$/Ag is depicted from the linear *I-V* plots of the device. These ohmic contacts can offer a free flow of charge carriers from active detector material to Ag electrodes, which generates high photocurrent in photodetectors, and they are also desirable for the study of intrinsic optoelectronic properties of materials [39].

Outstanding light-matter interaction is observed when current is observed to be increased when the device is illuminated in $Cu_{0.2}Sn_{0.8}Se$ nanoparticles thin film [40]. The photoresponse was studied with the help of Keithley 4200 SCS by switching the light periodically on and off. Fig. 4(c) shows the current of the device as a function of time at a constant biasing voltage of 1.5 V and under 670 nm light of power intensity 3mW/cm^2. Turning the light on, the current is seen to be enhanced through the device, and current steeply falls as the illumination is turned OFF unveiling repeatable and steady response towards the light. The apparent rise in current as the device is illuminated ascribed to the effective separation of the electron-hole pair, and it also confirms the semiconducting nature of grown crystal [41, 42].

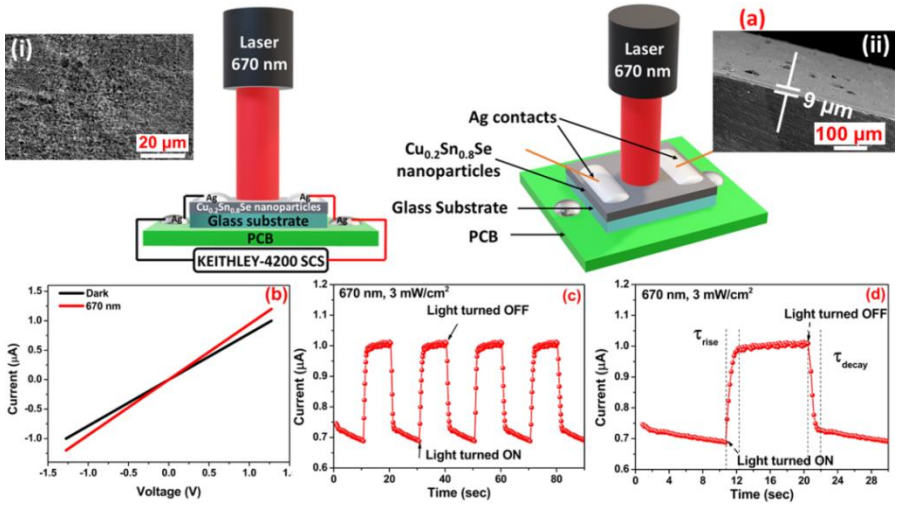

Fig. 4 – (a) Schematic diagram of photodetector based on $Cu_{0.2}Sn_{0.8}Se$ nanoparticles thin film (b) current-voltage characteristics of a photodetector in dark and illuminated condition (inset (i) shows the nanoparticle film (ii) shows cross-sectional image of the film), (c) photoresponse with 670 nm light, 3 mW/cm² and (d) magnified image of photoresponse of photodetector based on $Cu_{0.2}Sn_{0.8}Se$ nanoparticles thin film

Table 1 – Comparison of response times of $Cu_{0.2}Sn_{0.8}Se$ nanoparticles thin film based photodetector with reported TMC and TMDC materials.

Sample	Rise time	Decay time	References
SnS_2 nanosheets	20 s	31 s	43
WS_2 thin film	4.1 s	4.4 s	42
MoS_2 nanosheets	20 s	10.97 s	44
SnSe thin film	8.2 s	5.3 s	45
SnSe nanorods	3 s	3 s	46
Nb_2O_5 nanoplate	28 s	12 s	47
SnSe single crystal	2 s	2.5 s	39
$Cu_{0.2}Sn_{0.8}Se$ nanoparticle thin film	1.9 s	1.9 s	Present work

The good rise in the current and repeatable performance of the device resembles the good photoconducting behaviour of $Cu_{0.2}Sn_{0.8}Se$ nanoparticles-based device is understood from. The photocurrent ($I_{ph} = I_{ill} - I_{dark}$, where, I_{ill} is the current in illuminated condition, and I_{dark} is the dark current) of 0.32 μA is generated under illumination. The higher value of photocurrent is attributing the strong light-matter interaction in $Cu_{0.2}Sn_{0.8}Se$ nanoparticles. For quantitative analysis, detector parameters like photo responsivity, specific detectivity and external quantum efficiency are evaluated. The photoresponsivity ($R = I_{ph}/PS$, where, P is the power intensity of light and S is the active exposure area of device), specific detectivity ($D = RS^{1/2}/(2eI_{dark})^{1/2}$, where, e is the elementary charge, and I_{dark} is the current in dark condition) and external quantum efficiency ($EQE = hcR/e\lambda$, where, h is the Plank's constant, c is the speed of light and λ is the wavelength of illumination) are vital to assess performance of device and so they are calculated [42, 43]. The responsivity is found to be about 8.55 mAW^{-1}. The values of specific detectivity and external quantum efficiency are found to be about 2.04×10^9 Jones and 1.59 %, respectively. The response time is the essential parameter used to judge the switching performance of devices, and $Cu_{0.2}Sn_{0.8}Se$ nanoparticles-based devices are found to be a fast switching device with the very optimum response time when compared with other reported materials in Table 1. The rise time τ_{rise} is the required time for current rising to 90 % and decay time τ_{decay} is the required time for current falling to 10 %. The rise and decay time for photodetector are equal to 1.9 sec as seen from magnified image of time-resolved photocurrent as shown in Fig. 4(d). The high value of detector parameters and equal value of rising time and decay time are attributed to the good photoconducting behaviour of $Cu_{0.2}Sn_{0.8}Se$ nanoparticles thin film based photodetector [39].

4. CONCLUSION

The $Cu_{0.2}Sn_{0.8}Se$ nanoparticles are synthesised by high yield sonochemical exfoliation technique. The nanoparticles of lateral dimension 5-13 nm have excellent dispersibility. The exfoliated $Cu_{0.2}Sn_{0.8}Se$ nanoparticles have an orthorhombic structure with layers having space group P_{nma} having lattice parameters $a = 11.50$ Å, $b = 4.440$ Å and $c = 4.135$ Å. The lateral morphology of $Cu_{0.2}Sn_{0.8}Se$ nanoparticles is observed by transmission electron microscopy. The SAED pattern portrays the highly crystalline nature of nanoparticles. The detector is having a smooth surface and 9 μm thickness. The photodetector based on $Cu_{0.2}Sn_{0.8}Se$ nanoparticles thin film confirmed outstanding detection with a response time of 1.9 sec with photocurrent of 0.32 μA and enhanced photo-responsivity of 8.55 mA/W, detectivity of 2.04×10^9 Jones and EQE of 1.59 %. The response times are better than the previous reports on TMC and TMDC based photodetectors.

ACKNOWLEDGEMENTS

The author would like to thank the University Grants Commission, India, for providing Fellowship (NFO-2017-18-OBC-GUJ-54983). We thank DST, New Delhi for the assistance in general and the PURSE central facility Particle Size Analyzer and Zeta Potential Measuring System sponsored under PURSE program grant vide sanction letter DO. No. SR/Z-23/2010/43 dated 16th March 2011.

REFERENCES

1. Y. Pei, A.D. LaLonde, N.A. Heinz, G.J. Snyder, *Adv. Energy Mater.* **2**, 670 (2012).
2. M.T. Trinh, L. Polak, J.M. Schins, A.J. Houtepen, R.Vaxenburg, G.I. Maikov, G. Grinbom, A.G. Midgett, J.M. Luther, M.C. Beard, A.J. Nozik, M. Bonn, E. Lifshitz, L.D.A. Siebbeles, *Nano Lett.* **11**, 1623 (2011).
3. T. Siegrist, P. Merkelbach, M. Wuttig, *Annu. Rev. Condens. Matter Phys.* **3**, 215 (2012).
4. Y. Tanaka, Zhi Ren, T. Sato, K. Nakayama, S. Souma, T. Takahashi, Kouji Segawa, Yoichi Ando, *Nat. Phys.* **8**, 800 (2012).
5. G. Xiao, Y. Wang, J. Ning, Y. Wei, B. Liu, W.W. Yu, G. Zoua, B. Zou, *RSC Adv.* **3**, 8104 (2013).
6. D.-J. Xue, J. Tan, J.-S. Hu, W. Hu, Y.-G. Guo, L.-J. Wan, *Adv. Mater.* **24**, 4528 (2012).
7. B. Dong, C. Li, G. Chen, Y. Zhang, Y. Zhang, M. Deng, Q. Wang, *Chem. Mater.* **25**, 2503 (2013).
8. S. Shen, Y. Zhang, Y. Liu, L. Peng, X. Chen, Q. Wang, *Chem. Mater.* **24**, 2407 (2012).
9. S. Shen, Y. Zhang, L. Peng, Y. Du, Q. Wang, *Angew. Chemie Int. Ed.* **50**, 7115 (2011).
10. S. Shen, Q. Wang, *Chem. Mater.* **25**, 1166 (2013).
11. Z. Deng, D. Cao, J. He, S. Lin, S.M. Lindsay, Y. Liu, *ACS Nano* **6**, 6197 (2012).
12. D.K. Kim, Y. Lai, T.R. Vemulkar, C.R. Kagan, *ACS Nano* **5**, 10074 (2011).
13. R. Ulbricht, E. Hendry, J. Shan, T.F. Heinz, M. Bonn, *Rev. Mod. Phys.* **83**, 543 (2011).
14. X. Fang, Y. Bando, U.K. Gautam, C. Ye, D. Golberg, *J. Mater. Chem.* **18**, 509 (2008).
15. T. Zhai, L. Li, Y. Ma, M. Liao, X. Wang, X. Fang, J. Yao, Y. Bandoa, D. Golberga, *Chem. Soc. Rev.* **40**, 2986 (2011).
16. H.-W.Lee, P. Muralidharan, R. Ruffo, C.M. Mari, Y. Cui, D.K. Kim, *Nano Lett.* **10**, 3852 (2010).
17. K.Q. Peng, S.T. Lee, *Adv. Mater.* **23**, 198 (2011).
18. J. Ye, C. Zhang, C.-L. Zou, Y. Yan, J.G. Yong, S. Zhao, J. Yao, *Adv. Mater.* **26**, 620 (2014).
19. C. Liu, N.P. Dasgupta, P. Yang, *Chem. Mater.* **26**, 415 (2014).
20. I. Lefebvre, M. Szymanski, J. Olivier-Fourcade, J. Jumas, *Phys. Rev. B* **58**, 1896 (1998).
21. L. Makinistian, E.A. Albanesi, *phys. status solidi* **246**, 183 (2009).
22. B. Pejova, I. Grozdanov, *Thin Solid Films* **515**, 5203 (2007).
23. E. Barrios-Salgado, M.T.S. Nair, P.K. Nair, *ECS J. Solid State Sci. Technol.* **3**, Q169 (2014).
24. P.K. Nair, E. Barrios-Salgado, M.T.S. Nair, *phys. status solidi* **213**, 2229 (2016).
25. R.E. Abutbul, E. Segev, L. Zeiri, V. Ezersky, G. Makovab, Y. Golan, *RSC Adv.* **6**, 5848 (2016).
26. R.E. Abutbul, E. Segev, S. Samuha, L. Zeiri, V. Ezersky, G. Makov, Y. Golan, *Cryst. Eng. Commun.* **18**, 1918 (2016).
27. B. Pejova, A. Tanuševski, *J. Phys. Chem. C* **112**, 3525 (2008).
28. W.J. Baumgardner, J.J. Choi, Y.F. Lim, T. Hanrath, *J. Am. Chem. Soc.* **132**, 9519 (2010).
29. L. Li, Z. Chen, Y. Hu, X. Wang, T. Zhang, W. Chen, Q. Wang, *J. Am. Chem. Soc.* **135**, 1213 (2013).
30. S. Wu, C. Huang, G. Aivazian, J.S. Ross, D.H. Cobden, X. Xu, *ACS Nano* **7**, 2768 (2013).
31. A. Rogalski, J. Antoszewski, L. Faraone, *J. Appl. Phys.* **105**, 091101 (2009).
32. G. Konstantatos, E.H. Sargent, *Nat. Nanotechnol.* **5**, 391 (2010).
33. H. Tao, Y. Zhang, Y. Gao, Z. Sun, C. Yan, J. Texter, *Phys. Chem. Chem. Phys.* **19**, 921 (2017).
34. P. Pataniya, G.K. Solanki, C.K. Zankat, M. Tannarana, K.D. Patel, V.M. Pathak, *J. Mater. Sci. Mater. Electron.* **30**, 3137 (2019).
35. Q.H. Wang, K. Kalantar-Zadeh, A. Kis, J.N. Coleman, M.S. Strano, *Nat. Nanotechnol.* **7**, 699 (2012).
36. *Photodetectors (Materials, Devices and Applications)– 1st Edition*. (Woodhead Publishing: 2015).
37. R. Matsumoto, H. Hara, H. Tanaka, K. Nakamura, N. Kataoka, S. Yamamoto, A. Yamashita, S. Adachi, T. Irifune, H. Takeya, Y. Takano, *J. Phys. Soc. Jpn.* **87**, 124706 (2018).
38. S.A.B. Nashreen, F.P. Chetan, K.Z.M. Tannarana, G.K. Solanki, K.D. Patel, V.M. Pathak, P. Pataniya, *Mater. Sci. Semicond. Process.* **98**, 13 (2019).
39. K. Patel, G. Solanki, K. Patel, V. Pathak, P. Chauhan, *Eur. Phys. J. B* **92**, 200 (2019).
40. M. Tannarana, P. Pataniya, G.K. Solanki, S.B. Pillai, K.D. Patel, P.K. Jha, V.M. Pathak, *Appl. Surf. Sci.* **462**, 856 (2018).
41. M. Tannarana, G.K. Solanki, K.D. Patel, V.M. Pathak, P. Pataniya, *Bull. Mater. Sci* **42**, 79 (2019).
42. J.D. Yao, Z.Q. Zheng, J.M. Shao, G.W. Yang, *Nanoscale* **7**, 14974 (2015).
43. Y. Tao, X. Wu, W. Wang, J. Wang, *J. Mater. Chem. C* **3**, 1347 (2015).
44. Y. Chen, B. Lu, Y. Chen, X. Feng, *Sci. Rep.* **5**, 11505 (2015).
45. J. Cao, et al., *Nanotechnology* **25**, (2014).
46. A.S. Pawbake, S.R. Jadkar, D.J. Late, *Mater. Res. Express* **3**, 105038 (2016).
47. H. Liu, N. Gao, M. Liao, X. Fang, *Sci. Rep.* **5**, 7716 (2015).